Structure and magnetic properties of electrodeposited Ni films on n-GaAs(001)

2002 J. Phys.: Condens. Matter 14 12329

(http://iopscience.iop.org/0953-8984/14/47/308)

INSTITUTE OF PHYSICS PUBLISHING JOURNAL OF PHYSICS: CONDENSED MATTER

J. Phys.: Condens. Matter **14** (2002) 12329–12338 PII: S0953-8984(02)37230-8

Structure and magnetic properties of electrodeposited Ni films on n-GaAs(001)

C Scheck[1,2], P Evans[1], R Schad[1,2], G Zangari[1,3], J R Williams[4] and T F Isaacs-Smith[5]

[1] Center for Materials for Information Technology, University of Alabama, Box 870209, Tuscaloosa, AL 35487, USA
[2] Department of Physics and Astronomy, University of Alabama, Box 870324, Tuscaloosa, AL 35487, USA
[3] Department of Metallurgical and Materials Engineering, Box 870202, University of Alabama, Tuscaloosa, AL 35487, USA
[4] Department of Physics, Auburn University, Auburn, AL 36849, USA
[5] Space Research Institute, 231 Leach Science Center, Auburn University, Auburn, AL 36849, USA

Received 21 May 2002, in final form 2 October 2002
Published 15 November 2002
Online at stacks.iop.org/JPhysCM/14/12329

Abstract

We report the structural and magnetic properties of Ni films grown on GaAs(001) using electrodeposition, covering the thickness range 0–80 nm. The structure is characterized by mixed (001) and (011) epitaxial orientation of fcc Ni with a preference for the Ni(001) orientation. The magnetic anisotropy is originated by a combination of a crystalline contribution with fourfold symmetry and a uniaxial anisotropy probably caused by the asymmetry in the substrate surface structure. The saturation magnetic moment varies linearly with thickness, indicating limited intermixing between Ni film and GaAs substrate. This is ascribed to the low-energy deposition process characteristic of electrodeposition.

1. Introduction

The discovery of spin-dependent transport phenomena [1–3] has spurred investigations on the spin-dependent transport properties of various material combinations involving ferromagnetic materials (FMs). The proposal of creating active spin-electronic three-terminal devices with transistor-like characteristics [4] caused a still increasing interest in the integration of FMs with semiconductors. Such devices would require that electrons could be transferred between the FM and the semiconductor under conservation of the spin polarization [5]. Although diffusive transport with spin conservation appears unfeasible [6, 7], ballistic transport or tunnelling could conserve the electron spin. These effects might be achieved by forming a defined Schottky barrier at the FM/semiconductor. This interface would have to be chemically sharp at the atomic level and exhibit the least possible concentration of defects, features that are very

difficult to achieve. Most transition elements (including Ni, Fe and Co) react with silicon and form silicides even at room temperature [8, 9]. FM materials deposited on GaAs by evaporation or sputtering often show interdiffusion of Ga and/or As into the FM layer, which results in reduced magnetization values and increased resistivities [10–13]. More recent work showed that Fe intermixing with GaAs(001) substrates can be avoided by room temperature deposition while still obtaining good epitaxial growth [14, 15]. Spin-injection experiments using Fe layers on AlGaAs [16] also showed encouraging results.

A promising route to overcome the problem of interface intermixing might be the use of a deposition technique wherein the atoms to be deposited reach the substrate with very low energy. Electrodeposition is of interest in this respect, as it is a room temperature process which—as shown previously [17–20]—can yield high quality epitaxial layers.

In this paper we present the structural and magnetic properties of Ni films grown by electrodeposition directly onto the (001) surface of n-GaAs. In particular, we discuss the conditions upon which high quality, continuous films are obtained at low thickness.

2. Experimental details

The substrates were single crystalline GaAs(001), epi-ready and n-doped (carrier concentration 2×10^{17} cm^{-3}). The electrical back contact to the GaAs was made using a Ga (75%)–In (25%) eutectic which is liquid at room temperature. The area of deposition on the substrate for each sample was defined by covering the surface with an adhesive tape with a hole which exposed a surface area of 28.3 mm^2. Immediately prior to deposition, the substrates were etched for a duration of 2 min with a 10% NH_4OH solution. Electrodeposition was carried out under galvanostatic control (current density of 3.5 mA cm^{-2}) at 25 °C in a prismatic cell with vertical parallel electrodes using an EG&G model 273 A potentiostat. In order to reduce the effect of any resistance variation of the back contact to the substrate, galvanostatic deposition was preferred rather than potentiostatic. Graphite was used as the counter-electrode. Ni was deposited from a 0.1 M sulfate solution ($NiSO_4$) at pH = 2.5 without agitating the solution during deposition.

In-plane and out-of-plane preferred crystalline orientations were characterized by x-ray diffraction (XRD) using a Philips MRD system equipped with a Cu anode. Out-of-plane measurements were made as normal ω–2θ scans (or with a slight ω offset) using a focusing mirror which also acts as a monochromator. In-plane measurements were made as ϕ scans (sample rotation around its normal) at grazing incidence (ψ about 88°) with the detector angle 2θ corresponding to the lattice parameter of the planes for which the orientation was to be estimated. Here a secondary graphite monochromator was used. Both monochromators reduce but do not entirely suppress the Cu Kβ wavelength.

The magnetic properties of the films were investigated using a vibrating sample magnetometer (VSM) for a field range up to 10 kOe with the field oriented in the film plane. The magnetic easy and hard directions were estimated through the dependence of the remanent magnetization on the angle enclosed between field direction and sample axis. Full hysteresis loops were measured at selected sample angles.

The Rutherford backscattering spectroscopy (RBS) measurements were performed using a tandem accelerator (6SDH-2 Pelletron) built by the National Electrostatics Corporation and equipped with an RF exchange ion source for the production of He ion beams. Scattered ions from a collimated, 2 mm diameter, 2 MeV He^+ beam were detected at a scattering angle of 170°. Energy loss analysis indicated what kind of atom the He^+ ion interacted with, thus allowing for identification and profiling of the sample material. The RBS spectra were analysed using the code RUMP [21].

3. Results and discussion

3.1. Thickness calibration

The thickness of the films was measured or calculated using three different methods: the nominal thickness (T_N) was obtained from Faraday's law, assuming 100% efficiency of the electrochemical reduction process; the magnetic thickness (T_M) was calculated from the total magnetic moment of the sample and the thickness at the centre of the sample was measured through RBS (T_{RBS}).

T_N was determined using the formula $T_N = [I \times t \times M]/[N_A \times 2e \times d \times A]$ with plating current I, deposition time t, atomic mass M, Avogadro's constant N_A, elementary charge e, metal density d and film area A. According to the electrodeposition process using Ni^{2+} ions, two electrons are necessary to reduce one Ni ion to its elementary form as an Ni atom in the film. This assumes a current efficiency of 100%, a condition which typically is not fulfilled. Hence, T_N gives an upper limit for the true film thickness.

The measurement of the saturation magnetization (M_S) allows an estimation of the actual thickness under the assumption that the deposited films show bulk properties with respect to both density ($d_{\mathrm{Ni}} = 8.908$ g cm^{-3}) and magnetic moment ($M_{\mathrm{Ni}} = 54.4$ emu g^{-1}) and no oxidation of the Ni surface so that $T_M = [M_S]/[M_{\mathrm{Ni}} \times d_{\mathrm{Ni}} \times A]$. The assumption of bulk properties should be asymptotically justified for large enough values of the film thickness. Either surface oxidation or interdiffusion at the interface to the substrate would reduce M_S. This effect would cause the strongest deviations for thin films. Surface oxidation cannot be easily avoided by adding a protective cap layer when using electrodeposition since a change of the material being deposited is far less trivial by electrodeposition than it is for evaporation or sputtering. Therefore, our films were exposed to air and necessarily oxidized. Often it is observed that thin films of 3d metals with a good crystalline order show a limited amount of oxidation (around 1–2 nm of the metal film being oxidized) which effectively prevents further oxidation over long time periods [22–26]. Ni films are known to form, upon exposure to oxygen/air, NiO, which is antiferromagnetic and insulating [25], or $Ni(OH)_2$ [27]. The thickness of the oxide layer formed saturates at a couple of monolayers [24, 26]. We observed that the magnetic moments measured did not change over time, suggesting that the oxidation product indeed forms a stable cover layer which should reduce the moments systematically by a fixed amount. Interface intermixing can potentially also lead to a reduction of M_S [10–13].

Figure 1 shows film thickness obtained from the three methods as a function of electrodeposition time. Both T_M and T_{RBS} linearly increase with deposition time but show thickness values clearly below T_N. The linear increase of the T_{RBS} indicates a constant growth rate. T_M also increases linearly in time. Under the assumption that for larger thickness values the Ni film magnetization assumes bulk properties, this would indicate that also for the thinner samples we do not observe a strong deviation from bulk properties as one would expect for significant intermixing [10] or oxidation. This point needs further verification and a quantification of the degree of surface oxidation.

The surprising difference in slope between T_M and T_{RBS} is caused by a small non-uniformity of the sample thickness. This is because during electrodeposition the current density at the sample edges is higher than at the sample centre, causing the edges to grow at a slightly faster rate. Since the 2 mm diameter He^+ beam used in the RBS measurements was aimed at the sample centre this technique effectively measured the thinner part of the sample. The magnetic measurements, however, integrate over the entire sample area leading to the consistently higher values of T_M as compared with T_{RBS}. Profilometer measurements performed on various samples for different thicknesses confirmed that all films appeared to be thicker at the edges than at their centre.

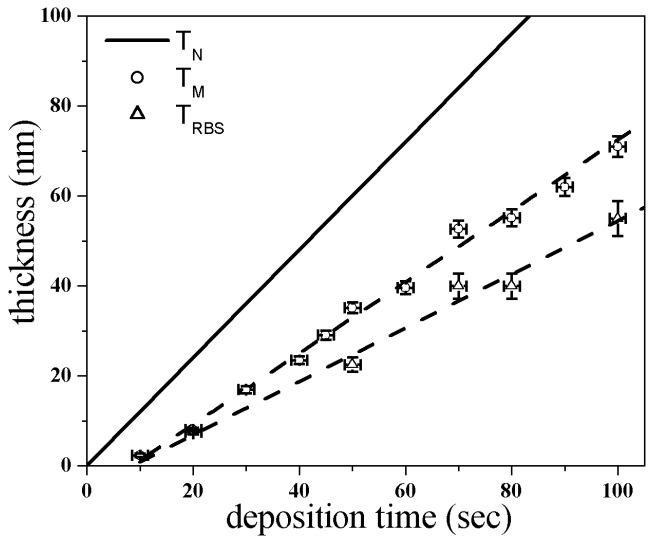

Figure 1. Thickness of electrodeposited Ni layers on GaAs(001) (nominal T_N, magnetic T_M and estimated by RBS T_{RBS}) as a function of deposition time. For definition of these three thickness values see the text. The dashed lines are linear fits to the data.

Comparing the nominal thickness T_N with T_M we find a current efficiency (for long deposition times >90 s) of $T_M/T_N = 58\%$.

All thicknesses quoted in the following are based on the RBS calibration. The growth rate is 0.59 nm s^{-1}. The linear extrapolations of both T_M and T_{RBS} intersect the x-axis (figure 1) at about 10 s. This delay in the deposition process is not untypical for electrodeposition and is ascribed to a capacitive charging current in the electrolyte/electrode system.

Structural properties

Figure 2 shows the high angle ω–2θ XRD scan for a 180 nm thick Ni film. In order to suppress the dominant GaAs(004) peak and its $K\beta$ satellite the sample angle ω was intentionally offset by 0.5°. A clear Ni(002) peak and a weaker (022) peak can be seen. The low signal levels are caused by a rather wide polar angular distribution of the crystal orientation with rocking curve widths of respectively 22° (002) and 8° (022). We find that the intensity ratios of (002) and (022) vary from sample to sample but with (002) always dominating. However, the most interesting point to note is the absence of the Ni(111) peak ($2\theta = 44.49°$), which would be the most intense peak for a completely untextured film and would also be expected as the texture of a non-epitaxial fcc film. This suggests that the films grow either with a texture unusual for fcc materials or that Ni grows epitaxially on n-GaAs(001). This was confirmed by in-plane XRD, where two preferred epitaxial growth relationships were observed. Figure 3 shows three ϕ scans for the detector angle 2θ set at the Ni(200), Ni(220) and Ni(111) peak positions, respectively. The ϕ scan with 2θ corresponding to the Ni(200) position shows four peaks with the Ni⟨100⟩ in-plane directions parallel to GaAs⟨110⟩. The ϕ scan with 2θ corresponding to the position of Ni(220) shows the Ni ⟨110⟩ to be aligned along the GaAs⟨100⟩ directions, i.e. enclosing an angle of 45° with the in-plane Ni⟨200⟩ directions. These two scans can be assigned to the first epitaxial relationship Ni(001)[100] ∥ GaAs(001)[110]. This corresponds to a 45° rotation of the fcc Ni structure with respect to the substrate, which has been reported previously for

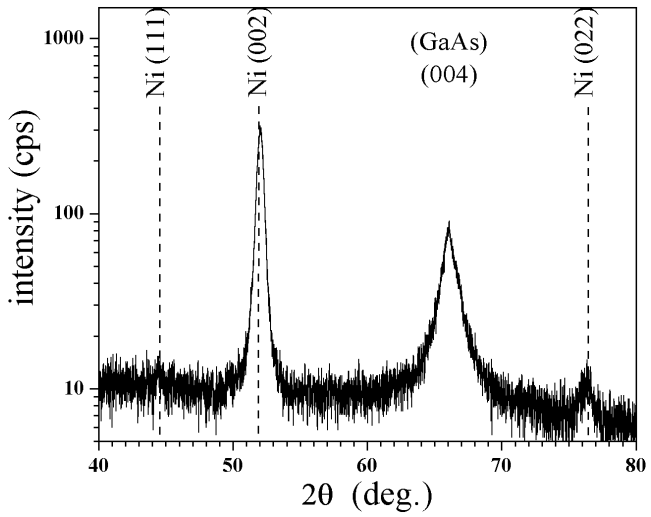

Figure 2. High angle ω–2θ x-ray measurement of a 180 nm thick Ni layer on GaAs(001). The vertical dashed lines indicate the 2θ peak positions of Ni(111), Ni(002) and Ni(022).

electrodeposited NiCu [17] and Cu [28] on GaAs(001). It should be noted that the Ni(001) orientation does not have any [111] in-plane direction; however, the (022) orientation does. The second epitaxial growth relationship is related to the Ni(022) peak seen in the ω–2θ scan (figure 2) combined with the Ni$\langle 111\rangle$ directions oriented along the GaAs[110] directions in-plane as shown in figure 3. The Ni(111) triplet peaks are characteristic of the four possible variants of having one of the in-plane Ni[111] directions aligned parallel to either GaAs[110] or GaAs[$1\bar{1}0$]. Indeed, in the Ni(011) surface the $\langle 111\rangle$ directions are at 109.5° to each other, whereas in the GaAs(001) surface the $\langle 110\rangle$ directions are at 90°, which leads to the four possible configurations, three of which are shown in figure 4. In (A) the Ni atoms are aligned with the GaAs[$1\bar{1}0$] direction whereas in (B) and (C) the Ni atoms are aligned along GaAs[110]. Cases B and C lead to a misalignment of the Ni atoms along the GaAs[$1\bar{1}0$] direction which gives rise to a triplet peak around GaAs[$1\bar{1}0$] (figure 3). However, the experimentally observed angle between the peaks in a triplet (10°, see figure 3) does not correspond with the theoretical angle between the Ni[111] and the GaAs[110] directions (19.5°). This might be due to some lattice deformation. It is interesting to note that the azimuthal mosaic spread (3° in figure 3) of the (001) epitaxy is much narrower than the polar mosaic spread (22°). Hence, the Ni layers have a rather well defined in-plane registry with the substrate while showing a wide spread in canting angle.

The (011) orientation of Ni layers electrodeposited on GaAs(001) had been reported previously [17, 20]. Here we find a mixture of Ni(001) and Ni(011) with, considering the substantially larger rocking curve width for Ni(001), dominantly Ni(001). In a previous study of electrodeposition of Ni on GaAs(001) as a function of current density [20] the authors report increasing peak intensities of (002) and (111) with decreasing current density. The current density used here (3.5 mA cm^{-2}) is lower than the range studied by Attenborough *et al* but the intensity of the (002) peak we find is not in disagreement with [20], given the different compositions and pH of the deposition solutions. Obvious, however, is the absence of the (111) orientation in our case (for all thicknesses) which might be due to the more complex plating solution composition used in [20]. Our XRD data do not show evidence for formation of bcc Ni as reported in [29].

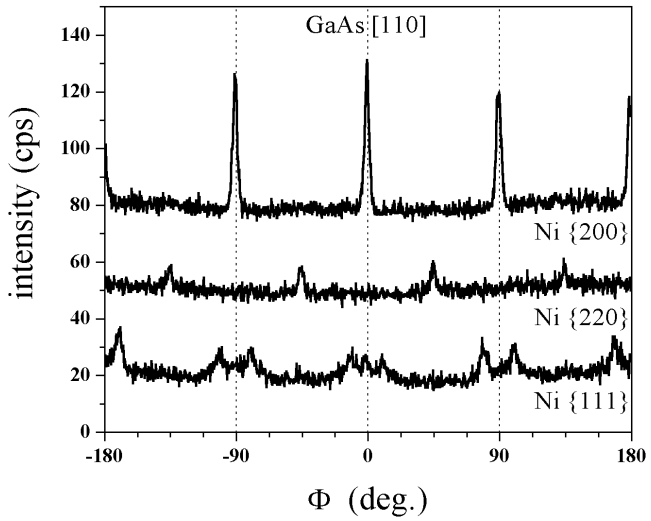

Figure 3. Grazing incidence XRD measurements of a 31 nm thick Ni layer on GaAs(001) with the scattering vector oriented at 88° from the sample normal. The detector angle was set to the position of respectively the Ni(200), Ni(220) and Ni(111) peaks for the three scans shown. The sample was rotated around the sample normal (ϕ rotation). $\phi = 0°$ corresponds to the GaAs[110] in-plane direction.

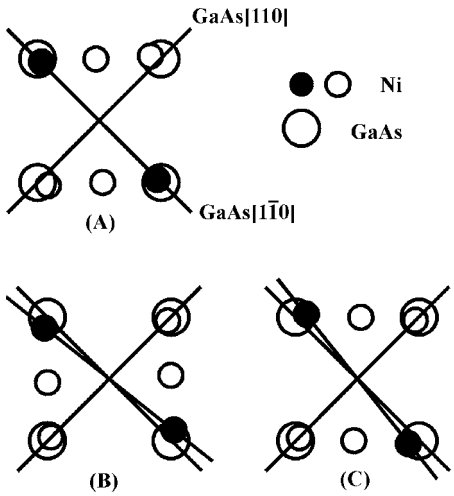

Figure 4. Three of the four possible alignments of the Ni(011) unit mesh on the GaAs(001) substrate. Only one of the Ni{111} directions can align with a GaAs{110} direction at a time.

In the following, in-plane directions will be stated with respect to the GaAs substrate axes because of the mixture of two crystalline orientations for the Ni films.

3.2. Magnetic properties

Figure 5 shows the remanence curves for respectively a 48 nm and a 19 nm thick Ni film. A dominant uniaxial anisotropy with the easy axis aligned parallel to the [110] direction of the

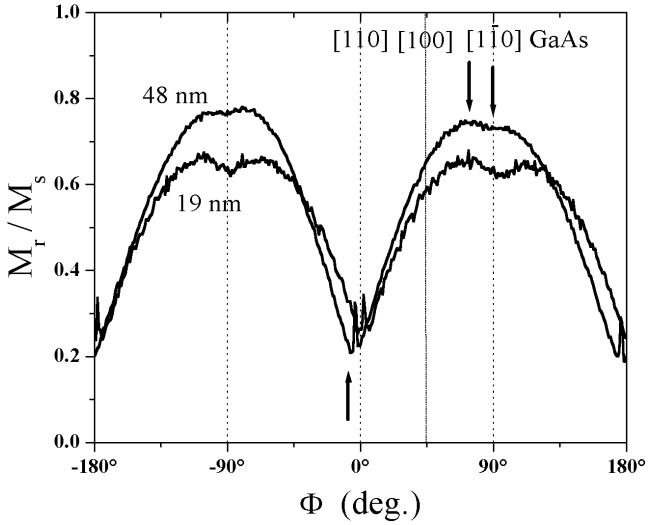

Figure 5. Remanence curves for a 48 nm and a 19 nm thick Ni film on GaAs(001). A value of the sample rotation angle ϕ equal to zero corresponds to a magnetic field direction parallel to GaAs[110]. The three arrows point to the characteristic positions of the remanence loops (hard axis, easy axis and almost-easy axis) for which individual hysteresis loops are shown in figure 6.

GaAs(001) surface can be seen. Superimposed on this is a fourfold anisotropy with the easy axis oriented about 65°–70° away from the GaAs[110] direction.

It is interesting to note the difference between the [110] and [1$\bar{1}$0] directions since these should be equivalent for an fcc Ni film with mixed (001) and twinned-(011) orientation. Such differences were observed previously for MBE grown Fe films on GaAs(001) [30] and were ascribed to the inequivalency of the bond directions along GaAs[110] and GaAs[1$\bar{1}$0]. The precise orientation of the easy axis direction varies slightly with thickness. With increasing Ni film thickness the dip in the remanence along GaAs[1$\bar{1}$0] does disappear and the easy axis direction moves from the GaAs[100] direction towards the [1$\bar{1}$0] direction. Additionally, the remanence curve loses structure, i.e. also the uniaxial anisotropy is reduced with increasing film thickness. The sharp peak in the remanence curve in the hard axis direction (along GaAs[110]) is reproducibly seen for all samples, a feature for which we currently cannot offer an explanation.

Figure 6 shows typical hysteresis loops for four different Ni film thicknesses. The loops were taken with the magnetic field oriented along the most prominent directions as found in the remanence curves for those films (indicated by arrows in figure 5) which were the hard and easy axis directions and the 'almost-easy' direction parallel to GaAs[1$\bar{1}$0]. For film thicknesses up to about 60 nm the easy axis loops are characterized by a high remanence or squareness which weakens for large values of the Ni thickness. The hard axis loop is most pronounced for intermediate thicknesses. For the thinnest and thickest films the hard axis loops show little difference from the easy axis loops. The thinnest films are certainly influenced by oxidation which should substantially alter the film magnetic properties. The oxidation product of Ni is $Ni(OH)_2$ [27] or NiO [24] which is antiferromagnetic and could lead to exchange biasing effects. Very thin antiferromagnetic layers are expected to only increase the coercivity rather than to cause a loop shift [31]. This pinning might dominate for the thinnest films allowing the clear anisotropy to develop only for thicker films. For thicker films the difference in loop shape between hard and easy axes tends to disappear. This would be in agreement with this anisotropy

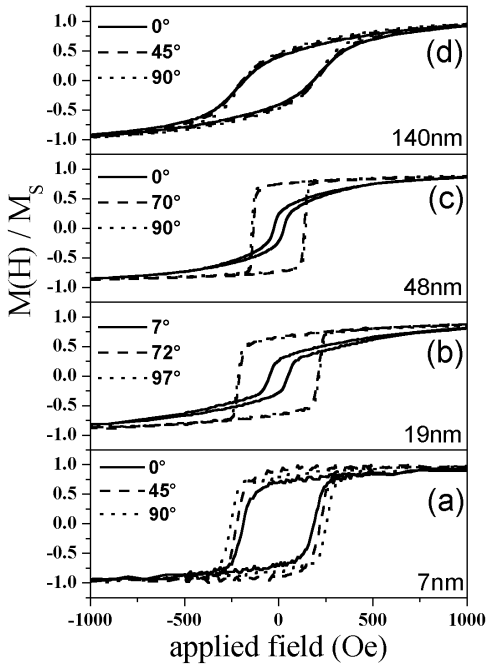

Figure 6. Hysteresis loops of four different Ni layers grown on GaAs(001) with thicknesses indicated in the graph. The measurements actually were extended to 10 kOe to ensure saturation of the films. Shown are only parts of these loops. Each graph does show three loops for each of which the orientation of the magnetic field with respect to the GaAs[110] direction is mentioned.

being caused by inequivalent GaAs[110] and [1$\bar{1}$0] substrate directions, the influence of which should decrease with increasing film thickness.

The coercivity for the three dominant directions presented in figure 6 is shown as a function of film thickness in figure 7. Easy axis coercivity values are in the range 150–250 Oe. The initial steep increase of H_c is probably due to islanding and possible relevant oxidation of the very thinnest films. Clearly visible is the most pronounced anisotropy (largest difference in H_c between easy and hard axis directions) in the intermediate thickness range which entirely disappears for larger thickness values. Disregarding the thinnest layer, as a general trend, the coercivity for all directions decreases with increasing Ni layer thickness which is not unusual for magnetic films [32–34]. Attenborough *et al* [20] reported a strong uniaxial anisotropy for Ni film electrodeposited on GaAs(001) using higher current densities. The data presented in [20] however do not rule out a crystalline contribution with fourfold symmetry since only two hysteresis loops are presented. However, the pH value of 3.9 used by Attenborough *et al* could be responsible for the absence of the crystalline contribution. We observed the disappearance of the crystalline anisotropy accompanied by a strengthening of the uniaxial anisotropy when depositing at pH 2.7 instead of pH 2.5. Films grown at pH 2.7 require about 2000 Oe to saturate in the hard axis direction. Growth at pH 2.3 shows a reduced current efficiency (38%) but results in similar magnetic properties as for pH 2.5. The values of the coercivities reported in [20] are similar to those shown here.

Epitaxial Ni(001) films grown on Cu(001) [35] and GaAs(001) [36, 37] had been reported to show an out-of-plane anisotropy which is ascribed to strain related effects [38]. Out-of-plane hysteresis loops measured on our samples confirm a clear in-plane anisotropy. However, the

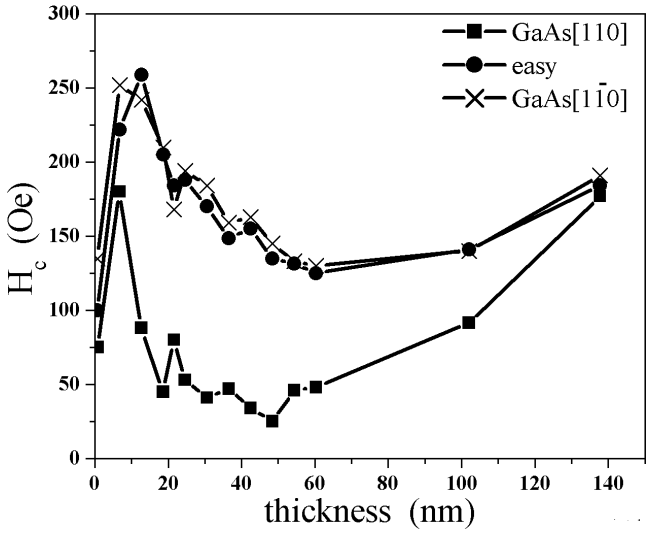

Figure 7. Coercivity H_c as a function of Ni layer thickness for three different orientations of the magnetic field as described in the text. The lines are a guide to the eye.

strength of the magnetic field necessary to saturate the samples in the out-of-plane direction is slightly (about 10%) below $4\pi M_s$ (as estimated from in-plane hysteresis loops) indicating the presence of anisotropy components favouring out-of-plane magnetization.

4. Conclusions

We have demonstrated growth of partially epitaxial Ni films on GaAs(001) using electrodeposition. The crystalline structure is characterized by a mixture of two phases, dominantly (001), and rather wide rocking curves.

The quality of the epitaxy of these films is not comparable to the structural quality of MBE grown Fe layers on GaAs. To some extent, this might be caused by the rather large lattice misfit between Ni and GaAs (12%) giving no orientation a clear preference above others. The magnetic properties show a clear anisotropy for the intermediate thickness range with contributions from crystalline components and uniaxial anisotropy leading to a mixed two- and fourfold symmetry, with the easy axis in plane for all thicknesses. The saturation magnetic moment increases linearly with thickness indicating limited interface intermixing between substrate and film due to the low-energy electrodeposition process.

The exact value of the pH of the electrolytic Ni solution is very important in determining the film magnetic properties. Films grown at lower pH (2.25) have similar magnetic properties whereas for higher pH (2.7) the fourfold in-plane anisotropy disappears and only a more pronounced uniaxial anisotropy remains.

Acknowledgments

This research was supported by NSF grant no ECS-0070236 and made use of NSF MRSEC shared facilities grant no DMR-98-09423.

References

[1] Binasch G, Grünberg P, Saurenbach F and Zinn W 1989 *Phys. Rev.* B **39** 4828
[2] Baibich M N, Broto J M, Fert A, Van Dau F N, Petroff F, Eitenne P, Creuzet G, Friederich A and Chazelas J 1988 *Phys. Rev. Lett.* **61** 2472
[3] Moodera J S, Kinder L R, Wong T M and Meservey R 1995 *Phys. Rev. Lett.* **7** 3273
[4] Datta S and Das B 1990 *Appl. Phys. Lett.* **56** 665
[5] Xu Y B, Freeland D J, Kernohan E T M, Lee W Y, Tselepi M, Guertler C M, Vaz C A F, Bland J A C, Holmes S N, Patel N K and Ritchie D A 1999 *J. Appl. Phys.* **85** 5369
[6] Lee W Y, Gardelis S, Choi B-C, Xu Y B, Smith C G, Barnes C H W, Ritchie D A, Linfield E H and Bland J A C 1999 *J. Appl. Phys.* **85** 6682
[7] Schmidt G, Ferrand D, Molenkamp L W, Filip A T and van Wees B J 2000 *Phys. Rev.* B **62** R4790
[8] Murarka S P 1983 *Silicides for VLSI Applications* (New York: Academic)
[9] Schad R, Jentzsch F and Henzler M 1992 *J. Vac. Sci. Technol.* B **10** 1177
[10] Rubinstein M, Rachford F J, Fuller W W and Prinz G A 1988 *Phys. Rev.* B **37** 8689
[11] Jonker B T, Krebs J J and Prinz G A 1988 *J. Appl. Phys.* **64** 5340
[12] Krebs J J, Jonker B T and Prinz G A 1987 *J. Appl. Phys.* **61** 2596
[13] Farrow R F C, Parkin S S P and Speriosu V S 1988 *J. Appl. Phys.* **64** 5315
[14] Xu Y B, Kernohan E T M, Freeland D J, Ercole A, Tselepi M and Bland J A C 1998 *Phys. Rev.* B **58** 890
[15] Zölfl M, Brockmann M, Köhler M, Kreuzer S, Schweinböck T, Miethaner S, Bensch F and Bayreuther G 1997 *J. Magn. Magn. Mater.* **175** 16
[16] Hanbicki A T, Jonker B T, Itskos G, Kioseoglou G and Petrou A 2002 *Appl. Phys. Lett* **80** 1240
[17] Allemand L, Froment M, Maurin G and Souteyrand E 1992 *Microsc. Microanal. Microstruct.* **3** 401
[18] Hart R, Midgley P A, Wilkinson A and Schwarzacher W 1995 *Appl. Phys. Lett.* **67** 1316
[19] Yi G and Schwarzacher W 1999 *Appl. Phys. Lett.* **74** 1746
[20] Attenborough K, De Boeck J, Celis J-P, Mizuguchi M and Akinaga H 1999 *IEEE Trans. Magn.* **35** 2985
[21] Doolittle L R 1985 *Nucl. Instrum. Methods Phys. Res.* B **9** 344
[22] Stierle A, Boedeker P and Zabel H 1995 *Surf. Sci.* **327** 9
[23] Schad R, Bahr D, Falta J, Beliën P and Bruynseraede Y 1998 *J. Phys.: Condens. Matter* **10** 61
[24] Saiki R S, Kaduwela A P, Osterwalder J, Fadley C S and Brundle C R 1989 *Phys. Rev.* B **40** 1586
[25] May F, Tischer M, Arvanitis D, Russo M, Hunter Dunn J, Henneken H, Wende H, Chauvistre R, Mårtensson N and Baberschke K 1996 *Phys. Rev.* B **53** 1076
[26] Wang W-D, Wu N J and Thiel P A 1990 *J. Chem. Phys.* **92** 2025
[27] de Jesus J C, Carrazza J, Pereira P and Zaera F 1998 *Surf. Sci.* **397** 34
[28] Zegenhagen J, Kazimirov A, Scherb G, Kolb D M, Smilgies D-M and Feidenhans'l R 1996 *Surf. Sci.* **346** 352
[29] Tang W X, Qian D, Wu D, Wu Y Z, Dong G S, Jin X F, Chen S M, Jiang X M, Zhang X X and Zhang Z 2002 *J. Magn. Magn. Mater.* **240** 404406
[30] Krebs J J, Jonker B T and Prinz G A 1987 *J. Appl. Phys.* **61** 2596
[31] Zhao T, Fujiwara H, Zhang K, Hou C and Kai T 2002 *Phys. Rev.* B **65** 014431
[32] Miller K J 1928 *Phys. Rev.* **32** 689
[33] Li M and Wang G-C 2000 *J. Magn. Magn. Mater.* **217** 199
[34] Meng H, Ong C K, Lim H S, Fang H C and Feng Y P 2000 *J. Magn. Magn. Mater.* **213** 37
[35] Gabriel B, Ballentine C A, Inglefield H E, Thompson C V and O'Handley R C 1996 *J. Appl. Phys.* **79** 5845
[36] Haque S A, Matsuo A, Yamamoto Y and Hori H 2002 *J. Magn. Magn. Mater.* **247** 117
[37] Przybylski M, Chakraborty S and Kirschner J 2001 *J. Magn. Magn. Mater.* **234** 505
[38] Uiberacker C, Zabloudil J, Weinberger P, Szunyogh L and Sommers C 1999 *Phys. Rev. Lett.* **82** 1289